



**HAL**  
open science

## Inside a Black Hole: the illusion of a Big Bang

Enrique Gaztanaga

► **To cite this version:**

| Enrique Gaztanaga. Inside a Black Hole: the illusion of a Big Bang. 2021. hal-03106344v7

**HAL Id: hal-03106344**

**<https://hal.science/hal-03106344v7>**

Preprint submitted on 22 Jul 2021

**HAL** is a multi-disciplinary open access archive for the deposit and dissemination of scientific research documents, whether they are published or not. The documents may come from teaching and research institutions in France or abroad, or from public or private research centers.

L'archive ouverte pluridisciplinaire **HAL**, est destinée au dépôt et à la diffusion de documents scientifiques de niveau recherche, publiés ou non, émanant des établissements d'enseignement et de recherche français ou étrangers, des laboratoires publics ou privés.

# Inside a Black Hole: the illusion of a Big Bang

Enrique Gaztañaga<sup>\*</sup>

*Institute of Space Sciences (ICE, CSIC), 08193 Barcelona, Spain  
Institut d'Estudis Espacials de Catalunya (IEEC), 08034 Barcelona, Spain*

July 17, 2021

## ABSTRACT

Black Hole (BH) and Big Bang (BB) solutions to classical General Relativity (GR) have mathematical singularities that make no physical sense. Moreover, the inside of the event horizon,  $r_{SW} = 2GM$ , for a BH with mass  $M$ , can not be modeled as regular matter/radiation. Yet, BH of different  $M$  have been observed. What is inside  $r < r_{SW}$ ? Our universe accelerates because it is trapped inside  $r < r_{\Lambda} = 1/H_{\Lambda} = (\Lambda/3)^{-1/2}$ , where  $\Lambda$  is an effective cosmological constant. What is outside  $r > r_{\Lambda}$ ? We present here a new non-singular solution to GR, which we call the BH Universe (BHU), that can model both a physical BH or a BB. The BHU consists of regular expanding matter/radiation and a false vacuum energy excess  $\Delta = \rho_{\Lambda} = \Lambda/8\pi G = \rho_{BH}$  so that  $r_{SW} = r_{\Lambda}$ . For the inside comoving observer the BHU is an homogeneous and isotropic expanding (FLRW) metric. For the outside observer, this same FLRW metric looks like a static BH with mass  $M \propto \Delta^{-1/2}$ . This frame duality allow us to connect two nested FLRW metrics as a new solution to GR and it also explains why our universe is expanding and not contracting. We discuss other distinct observational features of the BHU. For all we know, all observed BHs could just be BHUs. Observations of our universe are also consistent with a BHU, may be one of many, older and younger, interconnected island Universes.

**Key words:** Cosmology: dark energy, cosmic background radiation, cosmological parameters, early Universe, inflation

## 1 INTRODUCTION

A Schwarzschild BH metric (BH.SW) represents a singular object of mass  $M$ . The event horizon  $r_{SW} \equiv 2GM$  prevent us from interacting with the inside which makes BHs good Dark Matter candidates. Physically, a singular point does not make sense.<sup>1</sup> But objects with mass and sizes matching  $r_{SW}$  have been observed. What is the metric inside? What happens when they accrete matter or when two BHs merge? Do BHs grow and co-evolve with galaxies (e.g. [Kormendy & Ho 2013](#))? Do observed BH form in stellar collapse or are they seeded by primordial BHs? How do primordial BH form (e.g. [Kusenko & et al. 2020](#))? Most of these modelings assume the BH.SW solution, but can we actually answer any of this if we do not have a physical model for the BH interior?

Here, we look for an alternative solution to the BH.SW interior, defined as a non singular classical object of size  $r_{SW}$  which reproduces the BH.SW metric for the outside  $r > r_{SW}$ . A physical BH of size  $r < r_{SW}$  and mass  $M$ , has a density:

$$\rho_{BH} = \frac{M}{V} = \frac{3r_{SW}^{-2}}{8\pi G} = \frac{3M^{-2}}{32\pi G^3}. \quad (1)$$

This is more compact than any form of regular matter ([Buchdahl 1959](#)). The highest known density for a stellar object is that of a Neutron star, which has the density of an atomic nucleus, but is still a few times larger than  $r_{SW}$ . Yet BH of different  $M$  have been observed, even of galactic size. To achieve such a high density for

a perfect fluid, the radial pressure inside a BH needs to be negative ([Brustein & Medved 2019](#) and references therein). Cosmologist are used to this type of fluids, which are called Quintessence, Inflation or Dark Energy (DE). So, could the inside of a BH be DE? [Mazur & Mottola \(2015\)](#) have argued that the same DE repulsive force that causes cosmic acceleration could also prevent the BH collapse, resulting in the so call gravastar solution. The simplest DE is the ground state  $\rho_{vac} \equiv V_0(\varphi)$  of a scalar field  $\varphi(x)$ . [Gaztañaga \(2021b\)](#) have argued that a constant vacuum energy does not gravitate. But, as we will show here, a false vacuum (FV) discontinuity  $V = V_0 + \Delta$  does gravitate. We look for a classical BH solution defined by a spatial discontinuity at the event horizon. This requires non-static solutions with radial fluid velocity  $u \neq 0$  relative to the outside SW observer. The two key questions we want to address here are: What are possible metrics for the inside of such a physical BH? What is the meaning of the BH mass  $M$  measured by an outside SW observer, like us?

We find here a new solution to these questions, which we call the BHU metric. We will also explore the idea that our Universe corresponds to such BHU solution. As the universe expands  $H$  tends to  $H_{\Lambda}$  which corresponds to a trapped surface  $r_{\Lambda} = 1/H_{\Lambda}$ , just like the event horizon of a BH. Moreover, the density of our universe in that limit is  $\rho = 3H_{\Lambda}^2/8\pi G$  which corresponds to that of a BH, in Eq.1 for  $r_{SW} = r_{\Lambda}$ . This indicates that we actually live inside a very massive physical BH. It also tells us what is the metric inside a BH: our Universe is the only object whose interior we know and has the density of a BH. We will show that such situation is a solution to classical GR without singularities. This seems to avoid the singularity theorems in the lines pointed out by [Senovilla \(1998\)](#). But exact mathematical rigour is not the scope or concern of our paper, but rather a more physical and empirical approach to these issues.

<sup>\*</sup> E-mail: gaztanaga@gmail.com

<sup>1</sup> This is why it took Newton over 20 years to publish the inverse square law of gravity and re-invent integration on the way ([darkcosmos.com](#)).

The idea that the universe might be generated from the inside of a BH is not new and has extensive literature. [Easson & Brandenberger \(2001\)](#) and [Oshita & Yokoyama \(2018\)](#) present a good summary of past and recent literature which mostly focused in deSitter (dS) metric with a dual role of the BH interior and an approximation for our universe. Many of the formation mechanisms involve some modifications or extensions of GR (e.g. [Zhang 2018](#)), often motivated by quantum gravity or string theory. This is what we try to avoid here ([Ellis & Silk 2014](#)). There are also some examples (e.g. [Daghigh et al. 2000](#)) which presented models within the scope of a classical GR and classical field theory with FV interior similar to our BH.fv solution here. These models are affected by the no-go theorem, such as [Galtsov & Lemos \(2001\)](#), that state that no smooth solution to  $\varphi(x)$  can interpolate between dS and SW space. But this is not an issue for our solution for two reasons. First, the external asymptotic space is really SW+dS or FLRW (a BH is a perturbation within a FLRW metric), where solutions do exist (e.g. [Dymnikova 2003](#)). Second, we do not need  $\varphi(x)$  to smoothly transit between metrics:  $\varphi(x)$  is trapped in a FV, which is discontinuous by nature.

These previous works provide support to the idea that our universe could indeed be inside a BH, but often they are too simplistic, as they don't contain any matter or radiation. There are some papers that proposed the FLRW metric as BH interior. [Pathria \(1972\)](#) found that  $r_{SW}$  for a SW+dS metric behaves like  $R_{max}$  in a closed ( $k = +1$ ) FLRW metric, but [Knutsen \(2009\)](#) rightly pointed out the inconsistencies in notation and such interpretation. [Stuckey \(1994\)](#) found that a dust dominated FLRW universe could be mathematically joined to an outside BH.SW metric. This is a good precedent to our BH.u solution (in §4.2), but it did not include a  $\Lambda$  term, a FV vacuum, radiation or a physical interpretation. Our ideas are also quite different from [Smolin \(1992\)](#) who speculated that all final (e.g. BH) singularities 'bounce' or tunnel to initial singularities of new universes. Here we propose the opposite, that such mathematical singularities are not needed to explain the physical world. As stated by [Ellis \(2008\)](#), the concept of physical infinity is not a scientific one if science involves testability by either observation or experiment. The BHU model avoids the initial causal and entropy paradoxes ([Dyson et al. 2002](#); [Penrose 2006](#)) because of its origin within a larger spacetime.

In §2 we present our notation for Einstein field equations for perfect fluid and two homogeneous solutions: a FV and an expanding FLRW universe. In §3 we present a brief introduction to the general case of in-homogeneous solutions with spherical symmetry in proper SW coordinates. The FLRW solution can also be expressed in these coordinates. This duality is a key ingredient to find our solution for a physical BH interior. As far as we know this is a new result. In §4 we present two new solutions for the physical BH interior. In §5 we discuss how to apply these solutions to our universe. We end with a summary and a discussion of observational windows to test the BHU.

## 2 HOMOGENEOUS SOLUTIONS

We will solve Einstein's field equations (EFE) [Padmanabhan \(2010\)](#):

$$G_{\mu\nu} + \Lambda g_{\mu\nu} = 8\pi G T_{\mu\nu} \equiv -\frac{16\pi G}{\sqrt{-g}} \frac{\delta(\sqrt{-g}\mathcal{L})}{\delta g^{\mu\nu}}, \quad (2)$$

where  $G_{\mu\nu} \equiv R_{\mu\nu} - \frac{1}{2}g_{\mu\nu}R$  and  $\mathcal{L}$  is the matter Lagrangian. For perfect fluid in spherical coordinates:

$$T_{\mu\nu} = (\rho + p)u_\mu u_\nu + p g_{\mu\nu} \quad (3)$$

where  $u_\nu$  is the 4-velocity ( $u_\nu u^\nu = -1$ ),  $\rho$ , and  $p$  are the energy-matter density and pressure. This fluid is in general made of several

components, each with a different equation of state  $p = \omega\rho$ . For a fluid moving with relative radial velocity  $u$  with  $u^\nu = (u^0, u, 0, 0)$ , we have  $u_0^2 = -g_{00}(1 + g_{11}u^2)$  and:

$$\begin{aligned} T_0^0 &= -\rho - u^2(\rho + p)g_{11} & ; & & T_1^1 &= p + u^2(\rho + p)g_{11} \\ T_0^1 &= (\rho + p)u_0 u & ; & & T_2^2 &= T_3^3 = p \end{aligned} \quad (4)$$

For a comoving observer  $u = 0$ . The outside manifold  $\mathcal{M}_+$  is empty space so the solution  $g_+$  is the BH.SW. Because the inside  $\mathcal{M}_-$  is causally disconnected,  $\mathcal{M}_+$  acts like a simple boundary condition ([Gaztañaga 2021b](#)). Given some  $\rho$  and  $p$  inside  $r_{SW}$ , we will solve EFE inside with such boundary condition to find  $g_-$ . To impose the boundary at  $r_{SW}$  we will use the same (proper) SW coordinate frame that is not moving with the fluid so that  $T_0^1 \neq 0$ . This could result in solutions for  $\mathcal{M}_-$  that are not static. We will then verify [Israel \(1967\)](#) conditions to double check that the join manifold  $\mathcal{M} = \mathcal{M}_- \cup \mathcal{M}_+$  is also a solution to EFE and there are no surface terms (see §4.3). This is different from just matching two metrics. We will also find  $T_{\mu\nu}$  inside and outside the physical BH. This is not enough to find a physical solution to EFE. We also need to study its stability and find a causal formation mechanism.

### 2.1 Scalar field in curved space-time

Consider a minimally coupled scalar field  $\varphi = \varphi(x_\alpha)$  with:

$$\mathcal{L} \equiv K - V = -\frac{1}{2}\partial_\alpha\varphi\partial^\alpha\varphi - V(\varphi) \quad (5)$$

The Lagrange equations are:  $\bar{\nabla}^2\varphi = \partial V/\partial\varphi$ . We can estimate  $T_{\mu\nu}(\varphi)$  from its definition in Eq.2 to find:

$$T_{\mu\nu}(\varphi) = \partial_\mu\varphi\partial_\nu\varphi + g_{\mu\nu}(K - V) \quad (6)$$

comparing to Eq.3:

$$\rho = K + V \quad ; \quad p = |K| - V \quad (7)$$

In general we can have  $p_{\parallel} \neq p_{\perp}$  for non canonical scalar fields (see Eq.5 in [Díez-Tejedor & Feinstein 2006](#) for further details). The stable solution corresponds to  $p = -\rho \equiv -\rho_{vac}$ :

$$\bar{\nabla}^2\varphi = \partial V/\partial\varphi = 0 \quad ; \quad \rho \equiv \rho_{vac} = -p = V(\varphi) = V_i \quad (8)$$

where  $\varphi$  is trapped in the true minimum  $V_0$  or some false vacuum (FV) state  $V_i = V_0 + \Delta$ . The situation is illustrated in Fig.1.

The solution to Eq.2 for constant  $\rho = -p = V_i$  (without matter or radiation) for a general metric with spherical symmetry in proper coordinates (i.e. Eq.15) is given by dS metric in Eq.21 with  $H_\Lambda^2 \equiv 8\pi G\rho_\Lambda/3$  where  $\rho_\Lambda = V_i + \Lambda/8\pi G$ . This metric is static which indicates that the vacuum solution is in equilibrium. Quantum tunnelling can result in a phase transition or vacuum evaporation, which could break the equilibrium or result in slow evolution.

### 2.2 The FLRW metric in comoving spherical coordinates

The FLRW metric in comoving coordinates  $\xi^\alpha = (\tau, \chi, \delta, \theta)$ , corresponds to an homogeneous and isotropic space-time:

$$ds^2 = f_{\alpha\beta}d\xi^\alpha d\xi^\beta = -d\tau^2 + a(\tau)^2 \left[ d\chi^2 + \chi^2 d\omega_k^2 \right] \quad (9)$$

where we have introduced the solid angle:  $d\omega_k \equiv \text{sinc}(\sqrt{k}\chi)d\omega$  with  $d\omega^2 = \cos^2\delta d\theta^2 + d\delta^2$  and  $k$  is the curvature constant  $k = \{+1, 0, -1\}$ . For the flat case ( $k = 0$ ) we have  $d\omega_k^2 = d\omega^2$ . The scale factor,  $a(\tau)$ , describes the expansion/contraction as a function of

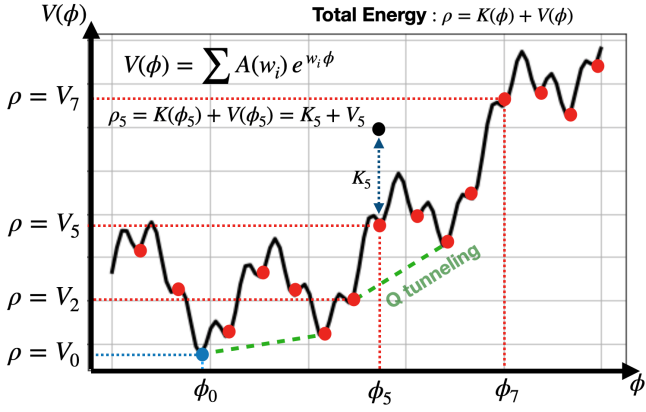


**Figure 1.** A potential  $V(\phi)$ , of a classical field  $\phi(x)$ , made of the superposition of 3 plane waves. A configuration with total energy:  $\rho = K + V$  (black dot at  $\phi_5$ ) can slowly loose its kinetic energy  $K_5$  (e.g. via Hubble damping) and relax into a static ( $K = 0$ ) ground state  $\rho = V_i \equiv V(\phi_i)$ ,  $i = 1, 2, 3$  (red dots), which we call false vacuum (FV) because they have an energy excess  $\Delta_i \equiv V_i - V_0$  with respect to the true vacuum at  $V_0 = V(\phi_0)$  (blue circle). A FV can be trapped inside other FV. Some FV are unstable or slow rolling, like  $\phi_7$ . Quantum tunneling (dashed green lines) allows  $\phi$  to jump between FV. A FV could also be reached by adding kinetical energy  $\delta K$  to the system to overcome the energy barrier where FV are trapped.

comoving or cosmic time  $\tau$  (proper time for a comoving observer). For a comoving observer, the time-radial components are:

$$\begin{pmatrix} T_{00} & T_{10} \\ T_{01} & T_{11} \end{pmatrix} = \begin{pmatrix} \rho(\tau) & 0 \\ 0 & p(\tau)a^2 \end{pmatrix} \quad (10)$$

i.e.  $u = 0$  in Eq.4. The solution to EFE in Eq.2 is:

$$3 \left( \frac{\ddot{a}}{a} \right) = R_{\mu\nu} u^\mu u^\nu = \Lambda - 4\pi G(\rho + 3p) \quad (11)$$

$$H^2 \equiv \left( \frac{\dot{a}}{a} \right)^2 = H_0^2 \left[ \Omega_m a^{-3} + \Omega_R a^{-4} + \Omega_k a^{-2} + \Omega_\Lambda \right] \quad (12)$$

$$\rho_\Lambda \equiv \rho_{\text{vac}} + \frac{\Lambda}{8\pi G} \quad (13)$$

$$\rho_c \equiv \frac{3H^2}{8\pi G} \quad ; \quad \Omega_X \equiv \frac{\rho_X}{\rho_c(a=1)} \quad (14)$$

where  $\Omega_m$  (or  $\rho_m$ ) represent the matter density today ( $a = 1$ ),  $\Omega_R$  is the radiation,  $\rho_{\text{vac}}$  represents vacuum energy:  $\rho_{\text{vac}} = -p_{\text{vac}} = V(\varphi)$  in Eq.8, and  $\rho_\Lambda = -p_\Lambda$  is the effective cosmological constant density. Given  $\rho$  and  $p$  at some time, we can use the above equations to find  $a = a(\tau)$  and determine the metric in Eq.9.

Eq.11 also corresponds to the geodesic acceleration (see Eq.43 bellow) and is valid for a perfect fluid in a more general metric. Note how  $p < -\rho/3$  (or  $\Lambda > 0$ ) produces acceleration (a repulsive gravity) and therefore expansion. This will be the physical mechanism that will avoid the BH singularity for the BHU solution.

During inflation,  $H$  was dominated by a vacuum field so that  $\rho_\Lambda \approx V(\varphi) \equiv 3H_\Lambda^2/8\pi G$ , which results in  $a \approx e^{\tau H_\Lambda}$ . Recent observations show that the expansion rate today is also dominated by  $\rho_\Lambda$ .<sup>2</sup> This indicates that the FLRW metric lives inside a trapped surface  $1/H_\Lambda = (8\pi G \rho_\Lambda/3)^{-1/2}$ , which behaves like the interior of a BH.

<sup>2</sup> This is no coincidence: the current late time cosmic acceleration can be understood as caused by inflation, see §5.1.

### 3 PROPER COORDINATES

The most general shape for a metric with spherical symmetry in proper or SW coordinates  $(t, r, \delta, \theta)$  is Padmanabhan (2010):

$$ds^2 = g_{\mu\nu} dx^\mu dx^\nu = -(1 + 2\Psi) dt^2 + \frac{dr^2}{1 + 2\Phi} + r^2 d\omega_k^2 \quad (15)$$

where  $d\omega_k$  was introduced in Eq.9 to allow for non-flat space.  $\Psi(t, r)$  and  $\Phi(t, r)$  are the two gravitational potentials. The Weyl potential  $\Phi_W$  is the geometric mean of the two:

$$(1 + 2\Phi_W)^2 = (1 + 2\Phi)(1 + 2\Psi). \quad (16)$$

$\Psi$  describes propagation of non-relativist particles and  $\Phi_W$  the propagation of light. For  $p = -\rho$  we usually get  $\Psi = \Phi = \Phi_W$ .

Eq.15 can also be used to describe the BH.SW solution (or any other solution) as a perturbation ( $2|\Phi| < 1$ ) around a FLRW background:

$$ds^2 \simeq -(1 + 2\Psi) dt^2 + (1 - 2\Phi) a^2 d\chi^2 + a^2 \chi^2 d\omega_k^2 \quad (17)$$

where  $r = a(\tau)\chi$  and  $t \simeq \tau$ . This same expression follows from perturbing the FLRW metric in Eq.9.

EFE for the general case of Eq.15 are well known, e.g. see Eq.(7.51) in Padmanabhan (2010). The case  $p = -\rho$  results in  $G_0^0 = G_1^1$ , and the solution is:

$$\Phi = \Psi = -G/r \int_0^r \rho(r) 4\pi r^2 dr - \Lambda r^2/6 - C_1/r \quad (18)$$

where  $C_1$  is an integration constant. The remaining EFE,  $G_2^2 = G_3^3$  are equivalent to energy conservation  $\nabla_\mu T_\nu^\mu = 0$ . For  $u = 0$ :

$$\partial_t \rho = -\frac{\rho + p}{1 + 2\Phi} \partial_t \Phi. \quad ; \quad \partial_r p = \frac{\rho + p}{1 + 2\Psi} \partial_r \Psi \quad (19)$$

Note how  $\rho = -p$  results in constant  $\rho$  and  $p$  everywhere, but with a discontinuity at  $2\Phi = 2\Psi = -1$  ( $r = r_{SW}$ ). This allows  $\rho$  and  $p$  to be constant, but different in both sides of  $2\Phi = 2\Psi = -1$ . One way to address this more formally is to study junction conditions (see §4.3). Another way around this, is to consider anisotropic pressure  $p_{\parallel} \neq p_{\perp}$  (Brustein & Medved 2019; Dymnikova 2019) which can result from non canonical scalar field Díez-Tejedor & Feinstein (2006). Empty space ( $\rho = p = \rho_\Lambda = 0$ ) in Eq.18 results in the BH.SW metric:

$$2\Phi = 2\Psi = -2GM/r \equiv -r_{SW}/r \quad (20)$$

where  $C_1 = GM$ . In the presence of  $\Lambda$ , the BH.SW metric corresponds to  $\rho_\Lambda = V(\varphi) + \Lambda/8\pi G = 0$  in Eq.8. Outgoing radial null geodesics cannot leave the interior of  $r_{SW}$ , while incoming ones can cross inside. The solution to Eq.18 for  $\rho = p = M = 0$ , but  $\rho_\Lambda \neq 0$  is the deSitter (dS) metric:

$$2\Phi = 2\Psi = -r^2 H_\Lambda^2 \equiv -r^2/r_\Lambda^2 \quad (21)$$

which is also static and has a trapped surface at  $r = r_\Lambda$  ( $2\Phi = -1$ ) where  $H_\Lambda^2 \equiv 8\pi G \rho_\Lambda/3$  and  $\rho_\Lambda = \Lambda/(8\pi G) + V(\varphi)$ . This metric corresponds to the surface of an sphere in a higher dimensional flat spacetime with a constant Ricci curvature  $R = 4\Lambda$ . This corresponds to a repulsive force, while Eq.20 is attractive (see Eq.43). The inside of  $r_\Lambda$  is causally disconnected, like the FLRW metric. Both metrics are equivalent for  $H = H_\Lambda$  (see Mitra 2012) which explains why the dS metric reproduces primordial inflation. The Steady-State Cosmology (SSC), with a perfect cosmological principle, is also reproduced by the same dS metric (O’Raifeartaigh & Mitton 2015). But contrary to the original SSC proponents (Bondi & Gold 1948; Hoyle 1948),  $\rho_\Lambda = V(\varphi)$  is trapped to a fixed value and there is no need for continuous creation of matter (C-field).

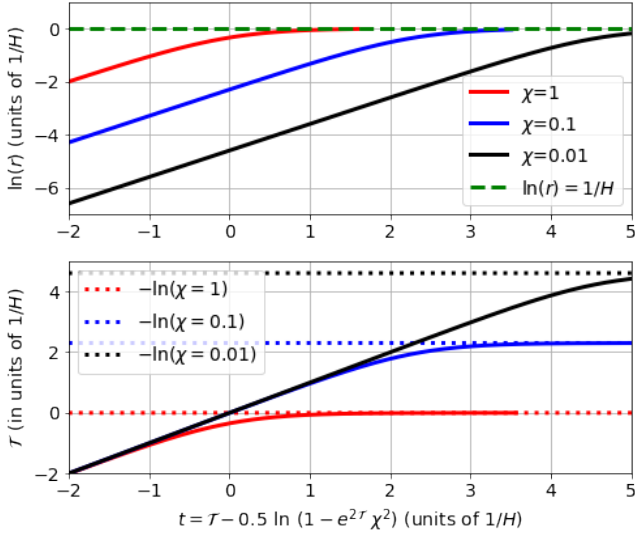


**Figure 2.** Logarithm of proper radius  $r = a(\tau)\chi$  (top) and comoving time  $\tau$  (bottom) as a function of SW time  $t$  in Eq.27 for  $a(\tau) = e^{\tau H_\Lambda}$  and different values of  $\chi$ . All quantities are in units of  $1/H_\Lambda$ . For early time or small  $\chi$ :  $\tau \simeq t$ . A fix  $\chi$  acts like an Horizon: as  $t \Rightarrow \infty$  we have  $\tau \Rightarrow -\ln \chi$  (dotted), which freezes inflation to:  $r = a\chi \Rightarrow e^{-\ln(H_\Lambda \chi)} \chi = 1/H_\Lambda$  (dashed).

When we express  $M = \rho V$  with  $V = 4\pi r^3/3$  and  $\rho = \rho_\Lambda$ , the BH.SW metric in Eq.20 becomes dS in Eq.21:

$$2\Psi = 2\Phi = -2GM/r = -8\pi G\rho_\Lambda r^2 = -H_\Lambda^2 r^2 \quad (22)$$

We will see this equation again soon (e.g. Eq.39). In comoving coordinates, dS singularity corresponds to a comoving Hubble horizon that shrinks to zero (see Fig.4). But note that this singularity can not be reached from the inside. Radial null events ( $ds^2 = 0$ ) connecting  $(0, r_0)$  with  $(t, r)$  follow:

$$r = r_{SW} \left( \frac{r_{SW} + r_0}{r_{SW} - r_0} e^{2t/r_{SW}} - 1 \right) / \left( \frac{r_{SW} + r_0}{r_{SW} - r_0} e^{2t/r_{SW}} + 1 \right) \quad (23)$$

so that it takes  $t = \infty$  to reach  $r = r_{SW}$  from any point inside. So the inside observer is trapped as in the FLRW case.

When we have both  $M$  and  $\rho_\Lambda$  constant everywhere, the solution to Eq.18 is:  $2\Phi = 2\Psi = -r^2 H_\Lambda^2 - r_{SW}/r$ , which corresponds to SW-dS metric, a BH in a dS background which has slightly shifted event horizon and is an approximation to our FLRW metric today.

### 3.1 The FLRW metric in proper coordinates

Consider a change of variables from  $x^\mu = [t, r]$  to comoving coordinates  $\xi^\nu = [\tau, \chi]$ , where  $r = a(\tau)\chi$  and angular variables  $(\delta, \theta)$  remain the same. The metric  $g_{\mu\nu}$  transforms to  $f_{\alpha\beta} = \Lambda_\alpha^\mu \Lambda_\beta^\nu g_{\mu\nu}$ , where  $\Lambda_\nu^\mu \equiv \frac{\partial x^\mu}{\partial \xi^\nu}$  is the Jacobian. Using the duality transformation :

$$\Lambda = \begin{pmatrix} \partial_\tau t & \partial_\chi t \\ \partial_\tau r & \partial_\chi r \end{pmatrix} = \begin{pmatrix} (1+2\Phi_W)^{-1} & a r H (1+2\Phi_W)^{-1} \\ r H & a \end{pmatrix}, \quad (24)$$

it is straightforward to verify that Eq.15, with  $2\Phi = -r^2 H^2$  and arbitrary  $a(\tau)$  and  $\Psi$ , transform into the FLRW of Eq.9:

$$f_{\alpha\beta} = \Lambda^T \begin{pmatrix} -(1+2\Psi) & 0 \\ 0 & (1+2\Phi)^{-1} \end{pmatrix} \Lambda = \begin{pmatrix} -1 & 0 \\ 0 & a^2 \end{pmatrix}, \quad (25)$$

In other words, these two metrics are the same:

$$-(1+2\Psi)dt^2 + \frac{dr^2}{1-r^2H^2} + r^2 d\omega_k^2 = -d\tau^2 + a^2 [d\chi^2 + \chi^2 d\omega_k^2] \quad (26)$$

So a generic spherically symmetric in-homogeneous metric can look like the homogeneous FLRW metric in comoving coordinates. And a general FLRW metric can be cast in proper coordinates. The expression for  $\Psi = \Psi(t, r)$  and  $t = t(\tau, \chi)$  or  $\tau = \tau(t, r)$ , depends on  $a(\tau)$ . For  $a(\tau) = e^{\tau H_\Lambda}$  (i.e.  $H = H_\Lambda$ ) we have  $\Psi = \Phi$  and

$$t = t(\tau, \chi) = \tau - \frac{1}{2H_\Lambda} \ln [1 - H_\Lambda^2 a^2 \chi^2], \quad (27)$$

where  $r < r_\Lambda = 1/H_\Lambda$ , which reproduces dS metric. In comoving coordinates the metric is inflating exponentially:  $a = e^{\tau H_\Lambda}$ , while in proper coordinates it is static. Fig.2 illustrates how this is possible and shows  $\tau = \tau(t, r)$  (see Mitra 2012 for some additional discussion). The remarkable frame duality of Eq.26, from a comoving time frame to a proper SW frame, is a new result as far as we know, and a key ingredient to interpret our new physical BH solution.

## 4 BLACK HOLE SOLUTIONS

### 4.1 False Vacuum Black Hole (BH.fv) solution

Eq.20 and Eq.21 are the simplest solutions to EFE. They both correspond to some form of empty space. We can use the same physical models to explore the simplest physical BH interior:

$$\rho = -p = \begin{cases} V_0 & \text{for } r > r_{SW} \\ V_0 + \Delta & \text{for } r < r_{SW} \end{cases} \quad (28)$$

where  $\Delta > 0$ . To recover BH.SW solution outside, we need  $\Lambda = -8\pi G V_0$  so that  $\rho_\Lambda = 0$ . But in a realistic situation, on larger scales the BH.SW metric should be considered a perturbation of FLRW background, e.g. Eq.17. It is straightforward (but tedious) to present the solution in this way. We take  $C_1 = 0$  in Eq.18 to avoid singular solutions. The solution to Eq.18 (which we called BH.fv) is then:

$$2\Phi = 2\Psi = \begin{cases} -r_{SW}/r & \text{for } r > r_{SW} \equiv 2GM \\ -r^2 H_\Lambda^2 & \text{for } r < r_{SW} = r_\Lambda \equiv 1/H_\Lambda \end{cases} \quad (29)$$

where:  $\rho_\Lambda = \rho_{BH} = \Delta$  and  $M = \frac{4\pi}{3} r_{SW}^3 \Delta$ . This has no singularity at  $r = 0$ . Note how, contrary to what happens in the BH.SW, in the BH.fv solution, the metric components don't change signature as we cross inside  $r_{SW}$ . In both sides of  $r_{SW}$  we have constant but different values of  $p$  and  $\rho$ . This comes from energy conservation in Eq.19. There is a discontinuity ( $\partial_r \rho = \infty$  and  $\partial_r p = \infty$ ) at  $2\Phi = -1$  where  $r = r_{SW}$ , in agreement with Eq.19, but the metric is static and continuous at  $r_{SW}$ . This solution only happens when  $r_{SW} = (8\pi G \Delta/3)^{-1/2}$ . The smaller  $\Delta$  the larger and more massive the BH. In the limit  $\Delta \Rightarrow 0$ , we have  $r_{SW} \Rightarrow \infty$  and we recover Minkowski space, as expected.

At a fixed location, the scalar field  $\varphi$  inside the BH is trapped in a stable configuration ( $\rho = V_0 + \Delta$ ) and can not evolve ( $K = 0$  in Eq.7). The same happens for the field outside (see Fig.1). A FV in Eq.28 with equal  $\Delta$  but with smaller initial radius  $r = R < r_{SW}$  is subject to a pressure discontinuity at  $r = R$  which is not balanced in Eq.19 and results in a bubble growth (Aguirre & Johnson 2005). Such boundary grows and asymptotically reaches  $R = r_{SW}$  (see top panel of Fig.2, Fig.3 and Eq.41). The inside of  $r_{SW}$  is causally disconnected, so the pressure discontinuity does not act on  $r = r_{SW}$ , which corresponds to a trapped surface.

## 4.2 Black Hole Universe (BH.u) solution

We will look next for solutions to the metric of Eq.15 where we also have matter  $\rho_m = \rho_m(t, r)$  and radiation  $\rho_R = \rho_R(t, r)$  inside:

$$\rho(t, r) = \begin{cases} -p = V_0 & \text{for } r > r_{SW} \\ V_0 + \Delta + \rho_m + \rho_R & \text{for } r < r_{SW} \end{cases} \quad (30)$$

with  $p = -V_0 - \Delta + \rho_R/3 \neq -\rho$  inside. This means  $\partial_t \Phi \neq 0$  and  $u \neq 0$ : the fluid inside has to move relative to SW frame of the outside observer<sup>3</sup>. For  $r > r_{SW}$ , the solution is the same as Eq.29. For the interior we define:  $2\Phi \equiv -r^2 H^2(t, r)$ , so that:

$$2\Phi(t, r) = \begin{cases} -r_{SW}/r & \text{for } r > r_{SW} = 2GM \\ -r^2 H^2(t, r) & \text{for } r < r_{SW} = 1/H_\Lambda \end{cases} \quad (31)$$

where  $r_{SW} = 2GM = 1/H_\Lambda$  as before. We can find the interior solution with a change of variables of Eq.24-26. The solution to Eq.31 is then  $H(t, r) = H(\tau)$ . Given some  $\rho(\tau)$  and  $p(\tau)$  in comoving coordinates in the interior of a BH we can use Eq.12 with  $\rho_\Lambda = \Delta = 3r_{SW}^2/8\pi G$  to find  $H(\tau)$  and  $a(\tau)$ . We call this a BH universe (BH.u). To complete the solution, i.e. to find  $\Psi$  and  $\tau = \tau(t, r)$ , we need to solve Eq.24 with  $2\Phi = -r^2 H^2(\tau)$ . For  $H(\tau) = H_\Lambda$  the solution is  $\Psi = \Phi$  and Eq.27. The flat FLRW metric with  $H = H_\Lambda$  becomes dS metric in Eq.21 as in the BH.fv solution.

Given  $T_{\mu\nu}$  in Eq.10 we can find  $\tilde{T}_{\alpha\beta}$  in the proper frame using the inverse matrix of Eq.24:  $\tilde{T}_{\alpha\beta} = (\Lambda^{-1})^\mu_\alpha (\Lambda^{-1})^\nu_\beta T_{\mu\nu}$ :

$$\tilde{T}_0^0 = -\frac{\rho - p2\Phi}{1 + 2\Phi} ; \quad \tilde{T}_1^1 = \frac{p - \rho2\Phi}{1 + 2\Phi} \quad (32)$$

which is independent of  $\Psi$ . Comparing to Eq.4 gives the velocity in the proper frame  $u^2 = -2\Phi = r^2 H^2$ , which is just the Hubble law. The Lorentz factor is  $\gamma = (1 + 2\Phi)^{-1/2}$  so that  $\gamma dr$  gives the proper length, in agreement with Eq.15.

Solution  $H(t, r) = H(\tau)$  in Eq.31 is valid for all  $r < r_{SW} = 1/H_\Lambda$  because  $H(\tau) > H_\Lambda$ . We can see this by considering outgoing radial null geodesic in the FLRW metric of Eq.9:

$$r_{out} = a(\tau) \int_\tau^\infty \frac{d\tau}{a(\tau)} = a \int_a^\infty \frac{da}{a^2 H(a)} < \frac{1}{H_\Lambda} = r_{SW} \quad (33)$$

which shows that signals can not escape from the inside to the outside of the BH.u. But incoming radial null geodesics  $a(\tau) \int_0^\tau \frac{d\tau}{a(\tau)}$  can in fact be larger than  $r_{SW}$  if we look back in time. This shows that inside observers are trapped inside the BH.u but they can nevertheless observe what happened outside (Gaztañaga & Fosalba 2021).

## 4.3 Junction conditions

We can arrive at the same BHU (BH.fv and BH.u) solutions using the junction conditions of Israel (1967). Here we follow closely the notation in §12.5 of Padmanabhan (2010). We will combine two solutions to EFE with different energy content, as in Eq.30, on two sides of a timelike hypersurface  $\Sigma = \mathcal{M}_- \cap \mathcal{M}_+$ . The inside  $g_-$  is FLRW metric (or dS metric for  $H = H_\Lambda$ ) and the outside  $g_+$  is BH.SW metric. This is similar to the case §12.5.1 in Padmanabhan (2010) with the difference that we use  $k = 0$  (instead of  $k = 1$ ) and consider a general FLRW solution  $a(\tau)$  with  $\Lambda$ ,  $\rho_m$  and  $\rho_R$  (instead of a pressure-free dust model without  $\Lambda$ ). This is relevant to provide the limiting trapped surface  $r_{SW} = \sqrt{3/\Lambda}$ . We define  $\Sigma$  to be fixed in comoving coordinates at  $\chi = r_{SW}$ , so  $\Sigma$  only depends  $\tau$  (here we fix  $a = 1$  when  $\chi = r_{SW}$ ). For the outside SW coordinate system,

$\Sigma_+$  is described by  $r = R(\tau)$  and  $t = T(\tau)$ , where  $\tau$  is the comoving time in the FLRW metric. We then have:

$$dr = \dot{R}d\tau ; \quad dt = \dot{T}d\tau, \quad (34)$$

where the dot refers to derivatives with respect to  $\tau$ . The induced metric  $h_-$  on the inside of  $\Sigma_-$  with  $y^a = (\tau, \delta, \theta)$  and fixed  $\chi = r_{SW}$ , is:

$$ds_{\Sigma_-}^2 = h_{-ab} dy^a dy^b = -d\tau^2 + a^2(\tau) r_{SW}^2 d\omega^2 \quad (35)$$

has to agree with  $h_+$ , the BH.SW metric outside at  $\Sigma_+$ :

$$-F dt^2 + F^{-1} dr^2 + r^2 d\omega^2 = -(F\dot{T}^2 - \dot{R}^2/F) d\tau^2 + R^2 d\omega^2 \quad (36)$$

where  $F = 1 - \frac{r_{SW}}{R}$ . The matching condition  $h_- = h_+$  is:

$$R(\tau) = a(\tau) r_{SW} ; \quad F\dot{T} = \sqrt{\dot{R}^2 + F} \equiv \beta(R, \dot{R}) \quad (37)$$

Thus, for a given FLRW solution  $a(\tau)$  we know both  $R$  and  $\beta$ . The extrinsic curvature  $K_\pm$  normal to  $\Sigma_\pm$  from each side is:

$$K_{-\tau}^\tau = 0 ; \quad K_{-\theta}^\theta = K_{-\delta}^\delta = -\frac{1}{ar_{SW}} \\ K_{+\tau}^\tau = \frac{\dot{\beta}}{R} ; \quad K_{+\theta}^\theta = K_{+\delta}^\delta = -\frac{\beta}{R} \quad (38)$$

Thus, the second matching condition  $K_- = K_+$  requires  $\beta = 1$ , which using Eq.37 results in:

$$\dot{R}^2 = R^2 H^2 = \frac{r_{SW}}{R} \quad (39) \\ \dot{T} = \frac{1}{1 - R^2 H^2} \Rightarrow T = \int \frac{dR}{HR(1 - H^2 R^2)} \quad (40)$$

This results in  $2\Psi = 2\Phi = -H^2 R^2 = -r_{SW}/R$  in the junction  $\Sigma$  (same as Eq.22 for  $H = H_\Lambda$ ). This is a generalization of dS space for arbitrary  $a(\tau)$ :  $2\Psi = 2\Phi = -R^2/r_H^2$  with  $r_H \equiv 1/H(\tau)$ . The critical density inside  $r_H$ , corresponds to that of a BH: from Eq.39 we have  $H^2 = r_{SW}/R^3 = 8\pi G\rho/3$ .

This  $\Sigma$  junction grows and tends to  $r_{SW} = 1/H_\Lambda$ . It takes  $T = \infty$  in the SW time of Eq.40 to asymptotically reach  $r_{SW} = 1/H_\Lambda$  (see Fig.2). In this limit, Eq.39 reproduces the BH.u junction of Eq.31 (and the BH.fv junction of Eq.29 for constant  $H = H_\Lambda$ ). Before that, the BHU junction is not static (not even in the SW frame) as  $H$  decays into  $H_\Lambda$  when  $R$  grows to  $r_{SW}$ . Despite the discontinuity in  $\rho$  at  $r_{SW}$ , the BHU metric and extrinsic curvature are continuous when we join them with the expanding timelike hypersurface of  $\Sigma$ . This proves that the BHU metric is also a solution to EFE and there are no surface terms in the junction (see Eq.21.167 in Misner et al. 1973). This does not require that both of the joined metrics have identical Riemann tensor or associated invariant scalars.<sup>4</sup> The  $\Lambda$  term corresponds to a trapped surface  $r_{SW} = 1/H_\Lambda$  in the FLRW (or dS) metric which matches the horizon of a BH in empty space (see Fig.5).

<sup>4</sup> This was questioned by two anonymous referees from Physical Review Letters (PRL), who recently rejected a preprint version of this same analysis (Gaztañaga 2021a). Ref-A found that these results warrant publication in PRL. Ref-B said: "I do not think the solutions presented are valid, and I still contend that a valid solution would require peculiar matter at the junction, which would be contrived". Ref-C agreed and added: "the Kretschmann scalar could reveal discontinuities" so the analysis "lacks a sufficiently firm foundation to be useful to research in this area". The solution to Eq.38 in Eq.39 demonstrates that there are no surface terms in  $\Sigma$ . The Kretschmann scalar is different for the BH.SW and FLRW metrics because  $T_{\mu\nu}$  is different, but this has nothing to do with the junction condition for  $\Sigma$ . ArXiv refused to publish this paper (as well as the preprint version of Gaztañaga 2020; Gaztañaga 2021b) because it "does not contain sufficient original or substantive scholarly research". This of course is just an unjustified opinion (see darkcosmos.com).

<sup>3</sup> This makes physical sense. Specially because the outside observer has no way to see inside. In general,  $T_{\mu\nu}$  could also be anisotropic.

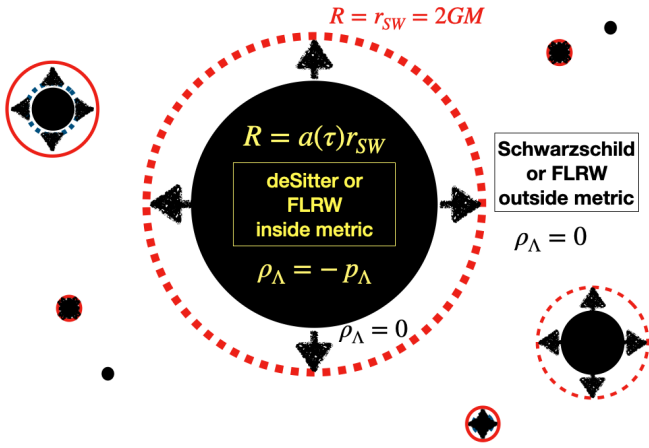


**Figure 3.** Illustration of the interior dynamics of a BHU. The junction  $R = a(\tau)r_{SW}$  (black disk) grows towards the SW radius  $R = r_{SW}$  (dashed red circle). The inside of  $R = a(\tau)r_{SW}$  is dS or a FLRW metric (dominated by negative pressure:  $\rho = -p$ ) while the outside is empty ( $\rho_\Lambda = 0$ ) BH.SW metric, a perturbation around a FLRW background with other BHs and matter.

#### 4.4 Evolving junction: internal BH dynamics

The junction conditions indicate that the division between interior and exterior solutions in Eq.29 and Eq.31 is not necessarily  $r_{SW}$ , which is the limiting case. This is illustrated in Fig.3. That both the metric and the external curvature are continuous at  $R$  shows that there are no surface terms and the join metric is a solution to EFE (see Eq.21.167 in Misner et al. 1973). The energy-momentum tensor  $T_{\mu\nu}$  corresponding to this solution has a discontinuity (as expected for a BH):  $\rho_\Lambda = -p_\Lambda \neq 0$  for  $r < R$  and  $\rho_\Lambda = 0$  for  $r > R$ .

Inside the physical BH we have an expanding junction:  $r = R(\tau) = a(\tau)r_{SW}$ . Because  $R(\tau) < r_{SW}$  is always inside  $r_{SW}$ , the external SW observer can not distinguish this evolving junction from the limiting static one  $r = r_{SW}$ . This is why we chose to express the solution this way. The junction  $R(\tau)$  grows and asymptotically tends to  $r_{SW}$  as shown in Fig.3. This happens at a finite comoving time  $\tau_\Lambda$  as in the top panel of Fig.2. The exact function depends on the form of  $a = a(\tau)$ . For constant  $\dot{a}/a = H = H_\Lambda = 1/r_{SW}$ , the solution can be expressed analytically as:

$$R(\tau) = R_0 e^{H_\Lambda \tau} = e^{H_\Lambda(\tau - \tau_\Lambda)} r_{SW} \quad (41)$$

where we have chosen  $a = 1$  when  $R = r_{SW}$ . We start with a finite size  $R = R_0 = a_0 r_{SW}$  at  $\tau = 0$ , where  $a_0 = e^{-\tau_\Lambda H_\Lambda}$ . After  $\tau_\Lambda H_\Lambda$  e-folds,  $R_0$  grows into  $R = r_{SW}$ . This inflation stops asymptotically at  $\tau = \tau_\Lambda = -r_{SW} \ln a_0$ . We can think of  $R_0$  as a quantum size (FV) fluctuation of energy  $\rho_\Lambda = \Delta$ , which (in empty space) will inflate to size  $r_{SW} = 1/H_\Lambda = (8\pi G\Delta/3)^{-1/2}$ .

This new solution to EFE is not just an arbitrary matching of two other random solutions. It is a new solution of a new physical configuration given by the energy content in Eq.30. This configuration corresponds exactly to our definition of a generic physical BH. The one we set to find in the introduction and whose horizon separates two regions with different matter-energy content. The same horizon defines the junction of two well known solutions to EFE.

## 5 IMPLICATIONS FOR OUR UNIVERSE

The BH.fv interior, dS metric, can be transformed into a FLRW metric with constant  $H = H_\Lambda$ . This frame duality provides a new

interpretation for the BH.fv solution in Eq.29. This is not only a solution for a BH inside a universe. The inside comoving observer, sees this solution as an expanding inflationary universe inside a BH, even when the metric is static in proper coordinates and  $r = r_{SW}$  is fixed. The same happens with the BH.u solution of Eq.31, which is equivalent to a child FLRW in the interior.

Recall how the outside BH.SW solution should be considered a perturbation of a parent FLRW in Eq.17. So we have two nested FLRW metrics which are connected with the BHU. Each one could have a different effective  $\rho_\Lambda$  (or FV). So could our universe be a child FLRW metric? The fact that we have measured  $\rho_\Lambda \neq 0$  provides a strong indication that this is the case. It is hard to explain what  $\Lambda$  means or the coincidence problem otherwise (see below).

The change of variables in Eq.24 is only valid for proper coordinates that are centered at the center of the BH location. But in the transformed (comoving) frame of Eq.26 any point inside is subject to the same expansion law with equal  $a(\tau)$ . From every point inside de BHU, comoving observers will see an homogeneous and isotropic space-time around them. At least all the way back in time to  $r_{SW} = 1/H_\Lambda$ , which is in their distant past. All points inside the BH were at the center in their distance past (just as in the homogeneous expanding universe). Even if all points inside see an homogeneous expansion, as they look back in time from a position that is off centered, some regions of the sky will be closer to the past horizon than others. This could result in some significant deviations from isotropy and homogeneity on the largest scales. Regions outside the trapped surface could see a similar background but with uncorrelated fluctuations that fit different parameters. Such deviations have already been measured in the form of large scale CMB anomalies and variations of cosmological parameters (see Fosalba & Gaztañaga 2021).

Note how we can have FVs inside other FVs (see Fig.1). So we can have BHs inside other BHs or FLRW metrics inside other FLRW universes. Mathematically this looks like a Matryoshka (or nesting) doll or a fractal structure. But physically, in the common SW frame, each BH has a different mass and therefore different physical properties. The child FLRW BHU have smaller mass (and larger FV) than the parent BHU. A BHU of one solar mass can have a FLRW metric inside but this inside will not have any galaxies and is going to be very different from that in a  $M \approx 5.8 \times 10^{22} M_\odot$  BHU, like ours, which contains billions of galaxies and BHs of many different sizes. So each BHU layer could be physically quite different from the next, unlike Matryoshka dolls or fractal structures.

### 5.1 The evolution of the BH universe

How did the universe evolve into the solution of Eq.31? This is an important question. It is not enough to find a solution to EFE. We need to make sure that such a configuration can be achieved in a causal way. Without  $\Lambda$ , the FLRW universe has no causal origin: the Hubble rate (in Eq.12) is the same everywhere, not matter how far, and this is not causally possible. The comoving coordinate  $\chi = r_{SW}$  that fixes the junction in §4.3 above can be identified as the causal horizon  $\chi_\S$  in the zero action principle (Gaztañaga 2021b). In the FLRW Universe, the Hubble Horizon  $r_H$  is defined as  $r_H = c/H$ . Scales larger than  $r_H$  cannot evolve because the time a perturbation takes to travel that distance is larger than the expansion time. This means that  $r > r_H$  scales are "frozen out" (structure can not evolve) and are causally disconnected from the rest. Thus,  $c/H$  represents a dynamical causal horizon that is evolving.

The standard evolution of our universe is shown in Fig.4. Note that here we choose  $a = 1$  now, as opposed to Fig.3 where  $a = 1$  corresponds to  $R = r_{SW}$ . It turns out that both are not so different

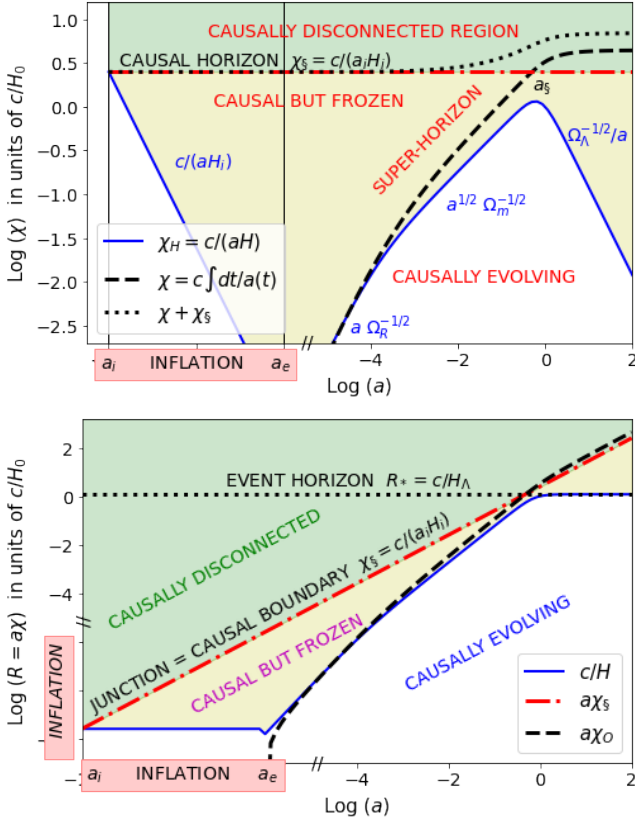


**Figure 4.** Comoving (top)  $\chi$  and proper (bottom)  $R = a(\tau)\chi$  coordinates in units of  $c/H_0$  as a function of cosmic time  $a$  (scale factor). The Hubble horizon  $c/H$  (blue continuous line), is compared to the observable universe  $a\chi_O$  after inflation (dashed line) and the primordial causal boundary  $\chi_s = c/(a_i H_i)$  (dot-dashed red line). Larger scales (green shading) are causally disconnected, smaller scales (yellow shading) are dynamically frozen and shrink to zero in comoving coordinates during dS phases. After inflation  $c/H$  grows again. At  $a \approx 1$  the Hubble horizon reaches our event horizon  $r_{SW} = c/H_\Lambda$ .

(the so call coincidence problem in cosmology). A primordial field  $\varphi$  settles or fluctuates into a false (or slow rolling) vacuum which will create a BH.fv with a junction  $\Sigma$  in Eq.35, where the causal boundary is fixed in comoving coordinates and corresponds to the particle horizon during inflation  $\chi_s = c/(a_i H_i)$  or the Hubble horizon when inflation begins. The size  $R = a(\tau)\chi_s$  of this vacuum grows and asymptotically tends to  $r_H = c/H$  following Eq.39 with  $H = H_i$ . The inside of this BH will be expanding exponentially  $a = e^{\tau H_i}$  while the Hubble horizon is fixed  $1/H_i$ . According to standard models of primordial inflation (Starobinskiĭ 1979; Guth 1981; Linde 1982; Albrecht & Steinhardt 1982), this inflation ends and vacuum energy excess converts into matter and radiation (reheating). This results in BH.u, where the infinitesimal Hubble horizon starts to grow following the standard BB evolution.

Note that the inflation in the BH.fv solution (i.e. Eq.41) stops naturally at cosmic time  $\tau_i = -H_i^{-1} \ln \chi_s H_i$  (see Fig.2) when proper distance is  $r = a(\tau)\chi_s = 1/H_i$ . In standard models of primordial inflation,  $H_i$  is much larger than  $H_\Lambda$  so that  $1/H_i$  is much smaller than  $1/H_\Lambda$ . So a quantum FV fluctuation  $\Delta$  only grows to a maximum size  $R = r_{SW} = (8\pi G\Delta/2)^{-1/2} = 1/H_i$ . Something else has to happen if we want the size to become cosmological. It could be reheating or some other mechanism. Quantum tunneling into smaller  $\Delta$  (see

Fig.1) also produces larger  $r_{SW}$ . Matter and radiation can also appear some other ways: from the original quantum fluctuations, quantum tunneling from/to other FV or infall of matter from outside (see §6.3-6.4). Regardless of these details,  $\chi_s$  remains the causal scale for the original BH.fv inflation in Eq.41. Recall that the BH.fv solution requires a discontinuity in  $\rho_\Lambda = 0$ , so this BH.fv evolution happens with independence of what we assume about  $\Lambda$  in EFE. A causal boundary in empty space generates a boundary term in the action that fixes the value of  $\Lambda$  to  $\Lambda = 4\pi G < \rho + 3p >$ , where the average is over the light-cone inside  $\chi_s$  (Gaztañaga 2021b). This  $\Lambda$  represents a trapped surface for the emerging BH.u universe.<sup>5</sup>

The observable universe (or particle horizon) after inflation is:

$$\chi_O = \chi_O(a) = \int_{a_e}^a \frac{d \ln a'}{a' H(a')} = \chi_O(1) - \bar{\chi}(a), \quad (42)$$

where  $a_e$  is the scale factor when inflation ends. For  $\Omega_\Lambda \approx 0.7$ , the particle horizon today is  $\chi_O(1) \approx 3.26c/H_0$  and  $\bar{\chi}(a) = \int_a^1 d \ln a' / (a' H)$  is the radial lookback time, which for a flat universe agrees with the comoving angular diameter distance,  $d_A = \bar{\chi}$ . The observable universe becomes larger than  $r_{SW} = r_\Lambda$  when  $a > 1$ , as shown in Fig.4 (compare dotted and dashed lines). This shows that, observers like us, living in the interior of the BH universe, are trapped inside  $r_{SW}$  but can nevertheless observe what happened outside. We can estimate  $\chi_s$  from  $\rho_\Lambda = < \rho_m/2 + \rho_R >$ , where the average is in the lightcone inside  $\chi_s$ . For  $\Omega_\Lambda \approx 0.7$  Gaztañaga (2021b) found:  $\chi_s \approx 3.34c/H_0$  which is close to  $\chi_O$  today. But imagine that  $\Omega_\Lambda$  is caused by some DE component and has nothing to do with  $\chi_s$ . We still have that  $\chi_s \lesssim \chi_O$ , because otherwise  $\chi_s$  would have cross  $RH = 1$  early on, resulting in smaller  $\chi_O$  than measured (see Fig.4).

Thus, at the time of CMB last scattering (when  $d_A \approx \chi_O$ ),  $\chi_s$  corresponds to an angle  $\theta = \chi_s/d_A \lesssim 1 \text{ rad} \approx 60 \text{ deg}$ . So we can actually observe scales larger than  $\chi_s$ . Scales that are not causally connected! This could be related to the so-called CMB anomalies (i.e. apparent deviations with respect to simple predictions from  $\Lambda$ CDM, see Planck Collaboration 2020b and references therein), or the apparent tensions in measurements from vastly different cosmic scales or times (e.g. Planck Collaboration 2020a).

## 6 DISCUSSION & CONCLUSION

We have looked for classical non-singular GR solutions for the BH interior. Our motivation is find a physical model and study if this results in some different properties for observed BHs. The outside manifold  $\mathcal{M}_+$  of a BH is approximated as empty space so the solution  $g_+$  is the BH.SW metric. Because the inside  $\mathcal{M}_-$  is causally disconnected,  $\mathcal{M}_+$  acts like a simple boundary condition. Given some  $\rho$  and  $p$  inside  $r_{SW}$ , we have solve EFE inside with such boundary condition to find  $g_-$ , the inside metric of a physical BH. To our surprise we have found that  $g_-$  is just the well known FLRW, the same metric that describes our universe! This frame duality, represented by Eq.24, has several observational consequences, as we will discuss below.

To impose the boundary at  $r_{SW}$  we have use the same (proper) SW coordinate frame that is not moving with the fluid so that  $T_0^1 \neq 0$ . This results in a solution for  $\mathcal{M}_-$  that is not static. We have verified Israel (1967) conditions to double check that the join manifold  $\mathcal{M}_- \cup \mathcal{M}_+$

<sup>5</sup> This picture changes if the fluctuation BH.fv happens within a non empty background. In such case we will just create a BH inside the larger universe, which is dominated by its own  $\Lambda$  and matter content. See §6.3 below.

is also a solution to EFE and there are no surface terms (see §4.3). This is different from just matching two random metrics. We have found  $T_{\mu\nu}$  inside and outside the physical BH and we have found what the BH mass  $M$  means (see §6.5 below).

A key point in these new solutions is the concept of FV energy (see §2.1 and Fig.1) and the fact that there is a FV or  $\rho_\Lambda$  discontinuity at  $r = r_{SW}$  (which could also be understood as a boundary to the Einstein-Hilbert action, *Gaztañaga 2021b*). The relativistic version of Poisson equation comes from the geodesic deviation equation (see Eq.12 in *Gaztañaga 2021b*):

$$\nabla_\mu \mathbf{g}^\mu = \frac{d\Theta}{ds} + \frac{1}{3}\Theta^2 = R_{\mu\nu}u^\mu u^\nu = \Lambda - 4\pi G(\rho + 3p) \quad (43)$$

where  $\mathbf{g}^\mu$  is the geodesic acceleration (*Padmanabhan 2010*). This is the same as the Raychaudhuri equation for a shear free, non-rotating fluid where  $\Theta = \nabla_\nu u^\nu$  and  $s$  is proper time. The above equation is purely geometric: it describes the evolution in proper time of the dilatation coefficient  $\Theta$  of a bundle of nearby geodesics. This is valid for a perfect fluid in a general metric. Note how  $p < -\rho/3$  (or  $\rho_\Lambda > 0$ ) produces acceleration (a repulsive gravity) and therefore expansion. This is the physical mechanism that explains how a FV (which has  $p = -\rho$ ) avoids the classical singularity theorems in GR (see *Senovilla 1998* and references therein). We can add both matter and radiation to both sides of  $r_{SW}$  and we still have a BHU solution. The BHU connects two FLRW metrics (see Fig.5).

### 6.1 False Vacuum BH solution (BH.fv)

BH.fv corresponds to constant FV discontinuity (Eq.28) with dS metric inside (Eq.29). dS metric has a trapped surface at  $r = r_{SW}$  which matches the BH.SW event horizon. A constant density (or negative pressure) corresponds to a centrifugal force,  $2\Phi = -(r/r_{SW})^2$  that opposes gravity,  $2\Phi = -r_{SW}/r$ , i.e. Eq.18. The equilibrium happens when both forces are equal, which fixes  $r = r_{SW}$ , and correspond to stable circular Kepler orbit. The BH mass  $M$  is just  $\rho_{BH} = \Delta$ .

Similar solutions have been known for a while (e.g. *Easson & Brandenberger 2001*; *Daghigh et al. 2000*; *Firouzjahi 2016*; *Oshita & Yokoyama 2018*; *Dymnikova 2019*), such as the gravastar (*Mazur & Mottola 2015*) or bubble/baby universes (*Aguirre & Johnson 2005*; *Kusenko & et al. 2020*). The BH.fv solutions here is not just a mere matching of the BH.SW and dS metrics, but a proper solution to Einstein's Field Equations (EFE) that fits our definition of a physical BH. We have also shown in §4.3 that there are no surface terms in the junction,  $\Sigma$ , which is a timelike expanding hypersurface. This is different from the gravastar model (which has matter in the surface) or the anisotropic models with negative radial pressure (*Brustein & Medved 2019*; *Dymnikova 2019*).

### 6.2 The BH universe solution (BH.u)

In our second solution (Eq.31), the BH interior is the FLRW metric. This BH.u solution is new, as far as we know. As discuss in the introduction, previous attempts were not proper solutions (*Pathria 1972*; *Knutsen 2009*) or did not include radiation or  $\Lambda$  (*Stuckey 1994*). We can have other BHs, matter and radiation inside a BHU within a larger space-time. The inside needs to be expanding as in the FLRW metric of Eq.9, with the same trapped surface given by  $\rho_\Lambda$ . This holds the expansion and balance gravity at  $r_{SW}$  as in the BH.fv solution. The join solution (Eq.31) is also a solution to Einstein's field equations as the two metrics reduce to the same form on a junction of constant  $\chi = r_{SW}$  in Eq.35, and the extrinsic curvature in Eq.38 is the same in both sides. The junction conditions indicate that the

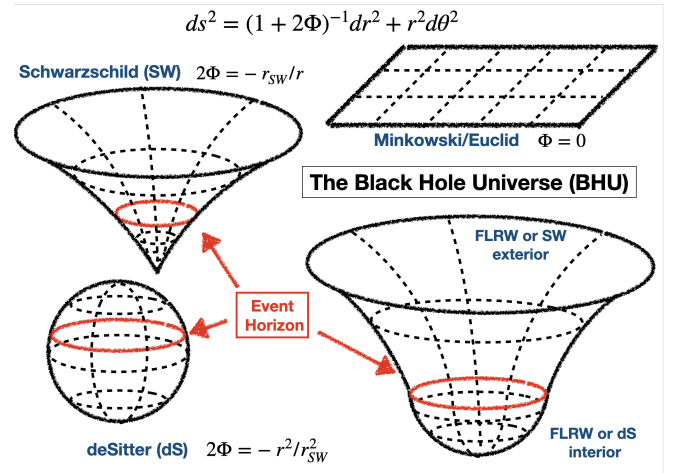


**Figure 5.** Spatial representation ( $dt = 0$ ) of  $ds^2 = (1 + 2\Phi)^{-1} dr^2 + r^2 d\theta^2$  for Minkowski ( $\Phi = 0$ , flat), Schwarzschild (SW,  $2\Phi = -1/r$ ), and deSitter (dS,  $2\Phi = -r^2$ ) metrics. Dashed lines show geodesics. The BHU solution has two nested FLRW metrics and no singularities.

division  $R(\tau)$  between interior and exterior solutions in Eq.29 and Eq.31 is not necessarily  $r_{SW}$ , which is the limiting case. The junction  $R(\tau)$  grows and asymptotically tends to  $r_{SW}$  as shown in Fig.3.

The exterior metric could also be FLRW, as the BH.SW metric can be considered a local perturbation within a larger FLRW background with arbitrary  $r = a(\tau)\chi$  in Eq.17. This is illustrated in Fig.5. In this case we need to distinguish between two different effective  $\rho_\Lambda$ , the one in the inside FLRW metric,  $\rho_\Lambda = \Delta$  and the one for the outside background, which should be smaller.

The solutions to the field equations are independent of the choice of coordinates but  $\tilde{T}_{\mu\nu}(t, r)$  depends on the fluid motion (see Eq.32). We used comoving coordinates  $(\tau, \chi)$ , where the fluid is expanding and the observed is comoving, to find the interior solution. But we can then transform back to proper SW frame  $(t, r)$ , using the duality transformation Eq.24, to find a full BH solution in Eq.31 that is continuous in the metric and curvature at  $r_{SW}$ , like in the BH.fv case. As in the singular BH.SW metric, outgoing radial null geodesics cannot escape the event horizon, but incoming ones can enter (see discussion around Eq.33). So the BHU solution is a physical BH.

### 6.3 BH formation

Another issue, which we only address partially here, is how such physical BH solutions can be achieved (e.g. astrophysical and primordial BH formation) and if they can have a causal origin. A local (quantum) fluctuation  $\Delta$  could generate a physical BH solution because either  $\varphi$  jumps into a FV or because of the zero action principle (see the Appollonian Universe in *Gaztañaga 2021b*). Hubble dumping of the kinetic energy  $K$  of a classical scalar field (see Fig.1) can also result in a FV trapped field configuration. Such initially small local discontinuity, with FV energy density  $\Delta$ , will grow as Eq.41 until it reaches BH size corresponding to  $\rho_{BH} = \Delta$ . So  $\Delta$  is the BH density: the smaller  $\Delta$  the larger the BH size and mass. Can we then make a very massive BH out of a quantum fluctuation, for free? There are some caveats to this. First, quantum fluctuation have a size given by  $\hbar$  so typical values of  $\Delta$  are much larger than  $\rho_\Lambda$  in our universe. Second, if  $\Delta$  is small, there is a chance that  $\varphi$  could tunnel back to the true vacuum (see Fig.1) before the BH grows to its SW radius  $r_{SW}$ .

Another caveat is that we have obtained these physical BH solutions for empty space outside (i.e. when  $\Phi$  is a small perturbation within a FLRW background of Eq.17). When  $r_{SW}$  and  $M$  become large compared to the background these solutions are not valid.

Could a BHU formed just from the final collapse of a dying star? Instead of a forming a BH singularity (as usually assumed), such collapse may just result into a large supernova (SN) explosion, where most of the stellar mass disappears in the SN and only a white dwarf or neutron star remains. Also a small BH could remain but it can not be a BH.SW because this is non physical. If such small BH is a BHU, quantum tunneling into smaller values of  $\Delta$  will make the BH grow as  $M \propto \Delta^{-1/2}$ . The SN explosion could also provide some kinetical energy  $\delta K = \Delta$  needed for  $\varphi$  to jump into a higher FV (see Fig.1), which will reduce  $M$ . This will trigger a BH.fv formation (so a new expansion in Eq.41). All these are speculation as we need more detail modeling to find how this happens. But the point we want to make is that the BH interior is important for models of BH formation and we can not just assume that a BH is a singular BH.SW metric inside, because this is not physical. In Fig.1 we can see that BHU of very different masses can be formed as the spectrum of  $\Delta_i$  values could be quite broad if we allow  $V(\varphi)$  to be a superposition of many plane waves. But, as we will show next, it is unlikely that BH mass can grow from accretion, as it is usually assumed for BH.SW.

#### 6.4 Gravitational Waves & Cosmic rays

Matter and radiation can infall inside the BHU solution. This results in a jump to the internal Hubble expansion rate ( $\Delta H/H = M_1/(2M_2)$ ). Such jump will be diluted away by the same internal expansion. This process is anisotropic by nature. So whatever we feed a BHU with, it is converted into internal kinetic expanding energy. For the outside SW frame this loss in the internal energy density,  $\rho$ , corresponds to BH mass loss,  $M$ , which could result in a Gravitational Wave (GW) and high energy cosmic rays, analogous to what happens during the Hubble damping in re-heating. The size of the signal could depend on the BHs spin and the anisotropy of the merging. If a BH or compact object of mass  $M_1$  is accreted to a larger BHU, with  $M_2 > M_1$ , the mass  $M_1$  behaves like dark matter. Within a Hubble time,  $M_1$  will be diluted away by the internal expansion of  $M_2$ , without change to its outside frame observed mass  $M_2$ . In a more general case, we could speculate that some of the energy from  $M_1$  could be transfer as kinetical energy  $\delta K$  to the  $\varphi_{M_2}$  field trapped in  $M_2$ , this  $\delta K$  could also be Hubble damped, as in reheating, into matter and radiation which will then also be diluted by the internal BH expansion of  $M_2$ . So again, no changes to  $M_2$ . Only when  $\delta K$  is large enough to overcome the FV barrier (see Fig.1) the merger could displace  $\varphi$  to different FV resulting in a new BH mass  $M$  larger than  $M_2$  but likely much smaller than  $M_2 + M_1$ :  $M_2 \lesssim M \ll M_2 + M_1$ . When  $M_1 = M_2$  with identical FV ( $\varphi_{M_1} = \varphi_{M_2}$ ) the final mass could be closer to  $M_1 + M_2$ .

Such BH binaries could provide observational evidence or rule out the BHU solution. In the SW frame, the BH mass  $M_2$  will first increase to  $M_2 + M_1$  and then decrease back to  $M_2 \lesssim M \ll M_2 + M_1$ . The upper bound corresponds to a typical mass loss rate in the merger (ignoring GW energy lost from spinning and ringdown). The mass  $M$  dilutes as  $a^{-3} \approx e^{-3H_2\tau}$ , for dS expansion (slower rate when both BH have similar mass), so that:

$$\frac{\partial M}{\partial \tau} \lesssim 3H_2 e^{-3H_2\tau} M_1 \quad (44)$$

where  $\tau$  is comoving time and  $H_2^{-1} = r_{SW} = 2GM_2$  is the internal Hubble rate of  $M_2$ . The external observer uses the SW frame ( $t, r$ ).

Using the inverse matrix of Eq.24 and Eq.27 we have:

$$\dot{M} \equiv \frac{\partial M}{\partial t} = \frac{\partial M}{\partial \tau} - \frac{rH}{1+2\Phi_W} \frac{\partial M}{\partial \chi} \lesssim 3H_2 e^{-3H_2t} M_1 \quad (45)$$

where we assumed that  $M$  does not vary with  $\chi$  and we are far from  $r_{SW}$ . This mass loss has to be compensated with some energy emission in the form of high energy cosmic rays or GW,  $e^{iw(r-ct)}$ . The typical amplitude  $|h|$ :

$$|h| = \frac{|\dot{h}|}{w} \approx \frac{2G\dot{M}}{wr} \lesssim 10^{-19} \left(\frac{M_1}{M_\odot}\right) \left(\frac{\text{Mpc}}{r}\right) \left(\frac{3H_2}{w}\right) e^{-3H_2t} \quad (46)$$

where  $r$  is the luminosity distance. The observed frequency  $f$ , if emitted at redshift  $z$  from us, is  $f = \frac{w}{2\pi(1+z)}$  so that:

$$f_2 \equiv \frac{3H_2}{2\pi(1+z)} = \frac{3(2GM_2)^{-1}}{2\pi(1+z)} \approx 100 \text{ KHz} \left(\frac{M_\odot}{M_2}\right) \frac{1}{1+z} \quad (47)$$

The characteristic amplitude spectral density strain is then:

$$2f^{1/2}|h(f)| \lesssim \frac{10^{-19} f^{-1/2}}{\pi(1+z)} \left(\frac{M_1}{M_\odot}\right) \left(\frac{\text{Mpc}}{r}\right) \left(\frac{f_2^2}{f_2^2 + f^2}\right)^{1/2} \quad (48)$$

which is within LIGO sensitivity (Buikema et al. 2020). So this predicts extra power with an exponential decay in the GW signal right after each detected GW ringdown (Carcasona & Gaztanaga, in preparation). This background is stronger at LISA mHz frequencies ( $M_2 \approx 10^7 M_\odot$ ). This GW background could also be observed in the CMB polarization (from tensor modes).

#### 6.5 What is $M$ for a physical BH?

The BH mass  $M$  in the BHU is given by the FV excess energy  $\Delta$ , so that  $\rho_{BH}$  in Eq.1 is  $\rho_{BH} = \Delta$  and  $M = (32\pi G^3 \Delta/3)^{-1/2}$ . So the larger  $\Delta$  the smaller the BH mass and size. This is independent of the matter and energy content that falls inside the BH (see §6.4). So  $M$  in the BHU solution does not correspond to the actual total mass or radiation inside, which is not observable from the outside, but should instead be interpreted in terms of the FV energy excess  $\Delta$ . This could have implications for models of astrophysical BH formation (such as Kormendy & Ho 2013) and primordial BH formation (e.g. Kusenko & et al. 2020 and references therein) which usually assume that BH accretion and merging results in linear increase of the BH mass  $M$ .

#### 6.6 Our universe as a BH

Both BH type solutions can be interpreted as a BH within our universe or as an expanding universe inside a larger space-time. As pointed out in the introduction, that the universe might be generated from the inside of a BH has a long and interesting history. Knutsen (2009) argued that  $p$  and  $\rho$  in the homogeneous FLRW solution are only a function of time (in comoving coordinates) and can not change at  $r = r_{SW}$  to become zero in the exterior. This is an important point and seems to contradict the BHU solution. The riddle is resolved with  $\Lambda$ . Without  $\Lambda$  the FLRW universe can not have a causal origin: the comoving density and Hubble rate are the same everywhere, and this is not causally possible. A causal horizon  $\chi_\S$  fixes  $\Lambda$  (Gaztañaga 2021b) which solves this problem and also generates an even horizon  $\chi_\S = r_{SW}$  similar to that of a BH.SW:  $r_{SW}$ . This allows for an homogeneous FLRW solution inside  $r_{SW}$  that has a  $\rho_\Lambda$  discontinuity at  $r_{SW}$  and looks in-homogeneous in the SW frame.

Homogeneity is therefore the illusion of the comoving observer inside  $r_\Lambda = r_{SW}$ . The FLRW metric is trapped inside  $r < r_\Lambda$ , and is then equivalent to an inhomogeneous spherically symmetric metric

of Eq.26. The FLRW metric is only homogeneous in space, but not in space-time. A new frame where comoving time and space are mixed, can break or restore this symmetry. The frame duality in Eq.24 is only valid for proper coordinates that are centered at the BH location. But in the transformed (comoving) frame any point inside the BHU is subject to the same expansion law with equal  $a(\tau)$ . From every point inside de BHU, observers will see an homogeneous and isotropic space-time around them. Just like in the universe around us.

### 6.7 Evidence for a BHU

We can sketch the evolution of our universe with this BHU model (see Fig.3-4). In proper coordinates this solution has no BB (or bounce): it is not singular at  $r = 0$  or at  $\tau = 0$ , because we have a non-singular BH.fv before we start the FLRW BH.u phase. The inside comoving observer is trapped inside  $r < r_{SW} = 2GM = 1/H_\Lambda$  and has the illusion of a BB. The space-time outside (the parent FLRW universe) could be longer and larger than the BB estimates. We could have a network of island universes with matter and radiation in between.

This also explains why our universe (or other island universes) is expanding and not contracting. The initial fluctuation  $H_i^2 = 8\pi G \Delta/3$  could be expanding ( $H_i > 0$ ) or contracting ( $H_i < 0$ ). In the later case it will either recollapse very quickly or it will else bounce into expansion dominated by the repulsive gravitational force that results from the negative pressure from constant  $\Delta$  or  $\Lambda$  (see Eq.43).

We have other observational evidence that the expanding metric around us is inside a BHU. We can recover the BB homogeneous solution in the limit  $\Delta \Rightarrow 0$ , where we have  $r_{SW} \Rightarrow \infty$  and  $\rho_\Lambda = 0$ . But we have measured  $\rho_\Lambda > 0$  ( $\Omega_\Lambda \approx 0.7$ ) which implies  $M \approx 5.8 \times 10^{22} M_\odot$  and  $r_{SW} \approx c/H_0$ , as in the BHU. The causal interpretation for  $\chi_8$ , also explains the observed coincidence between  $\rho_\Lambda$  and  $\rho_m$  today (Gaztañaga 2020; Gaztañaga 2021b).

If we look back to the CMB times,  $\chi_8$  corresponds to  $\approx 60$  degrees in the sky. The observed anomalies in the CMB temperature maps at larger scales (Gaztañaga 2020; Gaztañaga 2021b; Fosalba & Gaztañaga 2021; Gaztañaga & Fosalba 2021) provide additional support for the anisotropies expected in the BHU model. There is also a window to see outside our BHU using the largest angular scales for  $z > 2$  and measurements of cosmological parameters from very different cosmic times. There is already mounting evidence for this (e.g. Planck Collaboration 2020a; Riess 2019; Abbott et al. 2019).

If there are other island universes outside ours, Galaxies and QSO, as well as BHs, could be accreted from outside  $r_\Lambda$  into our BHU. Because the horizon  $1/H_\Lambda$  is so large, we can only see evidence of those mergers at early times, during or right after the CMB, when  $\chi_8$  subtends  $\approx 60$ deg. on the sky. Could this be related to rarely old QSO or galaxies observed at high  $z$ ? If our BHU merges with another BHU which is few % smaller, we might be able to see such % glitches in  $H(z)$  with current or future data, at  $z > 2$  and very large angle separation. Another possible observational evidence for the BHU solution is outgoing high energy cosmic rays or GW background signal from BH accretion or mergers within our BHU (see §6.4). High energy cosmic rays have been linked with X-ray binaries and AGNs, both hosting BH of different masses. Such GW background signal could also be observable as CMB tensor fluctuations.

Camacho & Gaztañaga (2021) found evidence for homogeneity and lack of correlations in the CMB at  $r > r_\Lambda$ . This suggests that the underlying physical mechanism sourcing the observed anisotropy encompasses scales beyond our causal universe. Fosalba & Gaztañaga (2021) found variations in cosmological parameters over large CMB regions. This is the largest reported evidence for a violation of the Cosmological principle. Such observations indicate a breakdown of

the standard BB picture in favor of the BHU. Their Fig.31 shows that the size of these regions follow the BHU relation between  $\chi_8$  and  $\rho_\Lambda$ . This is consistent with the idea that our universe was accreted to or created by a larger BHU.

### ACKNOWLEDGMENTS

This work has been supported by spanish MINECO grants PGC2018-102021-B-100 and EU grants LACEGAL 734374 and EWC 776247 with ERDF funds. IEEC is funded by the CERCA program of the Generalitat de Catalunya.

### DATA AVAILABILITY STATEMENT

The data and codes used in this article will be shared on request.

### References

- Abbott T. M. C., et al., 2019, *Phys. Rev. Lett.*, **122**, 171301  
Aguirre A., Johnson M. C., 2005, *Phys. Rev. D*, **72**, 103525  
Albrecht A., Steinhardt P. J., 1982, *Phys. Rev. Lett.*, **48**, 1220  
Bondi H., Gold T., 1948, *MNRAS*, **108**, 252  
Brustein R., Medved A. J. M., 2019, *Phys. Rev. D*, **99**, 064019  
Buchdahl H. A., 1959, *Phys. Rev.*, **116**, 1027  
Buikema A., et al., 2020, *Phys. Rev. D*, **102**, 062003  
Camacho B., Gaztañaga E., 2021, arXiv e-prints, p. arXiv:2106.14303  
Daghighi R. G., Kapusta J. I., Hosotani Y., 2000, arXiv:gr-qc/0008006,  
Diez-Tejedor A., Feinstein A., 2006, *Phys. Rev. D*, **74**, 023530  
Dymnikova I., 2003, *International Journal of Modern Physics D*, **12**, 1015  
Dymnikova I., 2019, *Universe*, **5**, 111  
Dyson L., Kleban M., Susskind L., 2002, *J. of High Energy Phys.*, **2002**, 011  
Easson D. A., Brandenberger R. H., 2001, *J. of High Energy Phys.*, **2001**, 024  
Ellis G., 2008, *Astronomy and Geophysics*, **49**, 2.33  
Ellis G., Silk J., 2014, *Nature*, **516**, 321  
Firouzjahi H., 2016, arXiv e-prints, p. arXiv:1610.03767  
Fosalba P., Gaztañaga E., 2021, *MNRAS*, **504**, 5840  
Galtsov D. V., Lemos J. P., 2001, *Classical and Quantum Gravity*, **18**, 1715  
Gaztañaga E., 2020, *MNRAS*, **494**, 2766  
Gaztañaga E., 2021a, pp <https://hal.archives-ouvertes.fr/hal-03106344>  
Gaztañaga E., 2021b, *MNRAS*, **502**, 436  
Gaztañaga E., Fosalba P., 2021, p. arXiv:2104.00521  
Guth A. H., 1981, *Phys. Rev. D*, **23**, 347  
Hoyle F., 1948, *MNRAS*, **108**, 372  
Israel W., 1967, *Nuovo Cimento B Serie*, **48**, 463  
Knutsen H., 2009, *Gravitation and Cosmology*, **15**, 273  
Kormendy J., Ho L. C., 2013, *ARA&A*, **51**, 511  
Kusenko A., et al. 2020, *Phys. Rev. Lett.*, **125**, 181304  
Linde A. D., 1982, *Physics Letters B*, **108**, 389  
Mazur P. O., Mottola E., 2015, *Classical and Quantum Gravity*, **32**, 215024  
Misner C. W., Thorne K. S., Wheeler J. A., 1973, *Gravitation*  
Mitra A., 2012, *Nature Sci. Reports*, **2**, 923  
O’Raifeartaigh C., Mitton S., 2015, p. arXiv:1506.01651  
Oshita N., Yokoyama J., 2018, *Physics Letters B*, **785**, 197  
Padmanabhan T., 2010, *Gravitation*, Cambridge Univ. Press  
Pathria R. K., 1972, *Nature*, **240**, 298  
Penrose R., 2006, Conf. Proc. C, 060626, 2759  
Planck Collaboration 2020a, *A&A*, **641**, A6  
Planck Collaboration 2020b, *A&A*, **641**, A7  
Riess A. G., 2019, *Nature Reviews Physics*, **2**, 10  
Senovilla J. M. M., 1998, *General Relativity and Gravitation*, **30**, 701  
Smolin L., 1992, *Classical and Quantum Gravity*, **9**, 173  
Starobinskiĭ A. A., 1979, *Soviet J. of Exp. and Th. Physics Letters*, **30**, 682  
Stuckey W. M., 1994, *American Journal of Physics*, **62**, 788  
Zhang T. X., 2018, *Journal of Modern Physics*, **9**, 1838